

## Supporting Information

# **An alcohol-soluble and ion-free electron transport material functionalized with phosphonate groups for solution- processed multilayer PLEDs**

*Bo Chen<sup>a, b</sup>, Lei Zhao<sup>a</sup>, Junqiao Ding<sup>a</sup>, Lixiang Wang<sup>a</sup>, Xiabin Jing<sup>a</sup> and Fosong Wang<sup>a</sup>*

<sup>a</sup> State Key Laboratory of Polymer Physics and Chemistry, Changchun Institute of Applied Chemistry, Chinese Academy of Sciences, Changchun, 130022, P. R. China

<sup>b</sup> University of Chinese Academy of Sciences, Beijing 100039, P. R. China

---

## Table of contents

1. General information	2
2. Device fabrication and characterization conditions	2
3. Synthesis	3
4. <sup>1</sup> H, <sup>13</sup> C and <sup>31</sup> P NMR spectra and MALDI-TOF mass spectrum of TPPO	5-8
5. Cyclic voltammetry plot of TPPO in acetonitrile solution	9
6. TGA and DSC curves of TPPO	10
7. Table of the photophysical, electrochemical and thermal properties of TPPO	11
8. AFM images of TPPO film before and after annealing	12
9. Device performance	13-18

---

## General Information

$^1\text{H}$  NMR spectra,  $^{13}\text{C}$  NMR and  $^{31}\text{P}$  NMR spectrum were recorded at room temperature on a Bruker Avance 300 NMR spectrometer.  $^{31}\text{P}$  NMR spectrum was referenced to external 85 %  $\text{H}_3\text{PO}_4$  (sealed in capillary tube, 0 ppm). Elementary analysis was carried on a Bio-Rad elemental analysis system. MALDI-TOF mass spectrum was performed on an AXIMA CFR MS apparatus (COMPACT). UV-visible absorption spectrum and photoluminescence spectrum was recorded on Perkin-Elmer Lambda 35 UV-vis spectrometer and Perkin-Elmer LS 50B spectrofluorometer, respectively. Thermal gravimetric analysis (TGA) and differential scanning calorimetry (DSC) were performed under a flow of nitrogen with Perkin-Elmer-TGA 7 and Perkin-Elmer-DSC 7 system, respectively, at a scanning rate of 10 °C/min. AFM characterization was performed on a SPA300HV with a SPI3800N controller (Seiko Instruments, Inc., Japan) in tapping mode. Cyclic voltammetry was performed on an EG&G 283 (Princeton Applied Research) potentiostat/galvanostat system. The sample was tested in 1 mM acetonitrile solution using ferrocene as reference under  $\text{N}_2$  atmosphere. The supporting electrolyte was 0.1 M tetrabutylammonium perchlorate ( $n\text{-Bu}_4\text{NClO}_4$ ), and the scanning rate was 100 mV/s.

## Device fabrication and characterization conditions

The substrates were commercial available indium tin oxide (ITO) coated glass with sheet resistance of 10  $\Omega$ /square. The substrates were pre-cleaned carefully, and treated by ozone for 25 min. The PEDOT:PSS solution was spin-coated onto the substrates with a thickness of 40 nm, and baked at 120 °C for 40 min in the air. After baking, the GPF chlorobenzene solution with a concentration of 12 mg/mL was spin-coated onto PEDOT:PSS at the 1.5 krpm for 1 min, and annealed at 80 °C for 30 min. Subsequently, the above TPPO layer was prepared by spin-coating the 6 mg/mL isobutanol solution at the 1.5 krpm for 1min. Except PEDOT:PSS, all the organic layers were assembled under nitrogen atmosphere. Finally, a 1-nm-thick film of LiF and a 100-nm-thick film of Al were vacuum-deposited onto the TPPO layer under the pressure of  $10^{-4}$  Pa, as required. The typical active area of the devices was 0.14 cm<sup>2</sup>. The device performance was tested at room temperature under ambient conditions. The EL spectra were measured by a PR650 spectra

colorimeter. The current - voltage and brightness - voltage curves of devices were measured by using a Keithley 2400/2000 source meter and a calibrated silicon photodiode.

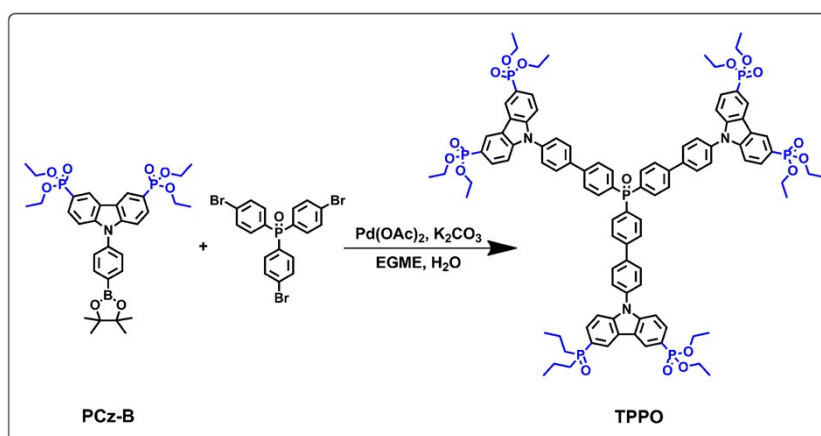
The electron mobility of the neat film was measured using the space-charge-limited-current (SCLC) method. The electron-only device configuration is ITO/Al (100 nm)/TPPO (90 nm)/ LiF (1 nm)/Al (100 nm). The current-voltage curve was recorded using a computer-controlled Keithley 2400 source meter. The electron mobility was calculated according to a simplified space-charge limited function:

$$J = \frac{9}{8} \varepsilon_0 \varepsilon_r \mu \frac{V^2}{L^3}$$

where  $J$  is the current density,  $\varepsilon_0$  is the permittivity of free space,  $\varepsilon_r$  is the relative permittivity of 3 for organic material,  $\mu$  is the zero-field mobility,  $V$  is the potential across the device,  $L$  is the thickness of active layer.

## Synthesis

All chemicals and reagents were used as received from commercial sources without further purification. Solvents for chemical synthesis were purified according to the standard procedures. The intermediates PCz-B[1] and tris(4-bromophenyl)phosphine oxide[2] were prepared according to the literature procedures.



**Scheme S1.** Synthetic route of TPPO.

**TPPO:** To the mixture solvent of 9 mL ethylene glycol mono methyl and 3 mL water, tris(4-bromophenyl)phosphine oxide (0.32 g, 0.63 mmol), PCz-B (1.33 g, 2.07 mmol) and K<sub>2</sub>CO<sub>3</sub> (0.48

---

g, 3.48 mmol) were added. After all the solid was dissolved, Pd(OAc)<sub>2</sub> (9.0 mg, 40.2 μmol) was added to the colorless solution. The color of the solution soon turned into dark brown. After the solution was stirred at r. t. for 3 hours, the solvent was removed by vacuum distillation. The residue solid was further purified by column chromatography on silica (200–300 mesh) with ethyl acetate/methanol ( $V_{\text{ethyl acetate}} : V_{\text{methanol}} = 20 : 1$ ). The final product was obtained as white solid (0.59 g, 52%). <sup>1</sup>H NMR (DMSO-d<sub>6</sub>, 300 MHz, δ): 8.88 (d, 6H,  $J = 13.6$  Hz), 8.13-8.08 (m, 12H), 7.97-7.83 (m, 18H), 7.60 (dd, 6H,  $J_1 = 3.0$  Hz,  $J_2 = 8.5$  Hz), 4.13-4.00 (m, 24H), 1.27 (t, 36H,  $J = 7.1$  Hz). <sup>13</sup>C NMR (DMSO-d<sub>6</sub>, 75 MHz, δ): 143.61 (d,  $J = 2.1$  Hz), 143.51, 139.90, 136.59, 133.46, 133.27 (d,  $J = 10.0$  Hz), 132.09, 130.77 (d,  $J = 11.8$  Hz), 129.86, 128.55, 128.25 (d,  $J = 12.0$  Hz), 126.37 (d,  $J = 10.9$  Hz), 123.18 (d,  $J = 17.5$  Hz), 122.08, 119.56, 111.34 (d,  $J = 15.5$  Hz), 62.43 (d,  $J = 5.2$  Hz), 17.10 (d,  $J = 5.9$  Hz). <sup>31</sup>P NMR (DMSO-d<sub>6</sub>, 121 MHz, δ): 26.15, 20.65. Anal calcd. For C<sub>96</sub>H<sub>102</sub>N<sub>3</sub>O<sub>19</sub>P<sub>7</sub>: C, 63.40; H, 5.65; N, 2.31; Found: C, 63.79; H, 5.98; N, 1.95. Calcd mass: 1818.7; MALDI-TOF mass found ( $m/z$ ): 1818.6 [ $M^+$ ], 1841.6 [ $M + Na^+$ ].

---

[1] Chen, B.; Ding, J. Q.; Wang, L. X.; Jing, X. B.; Wang, F. S. *Chem. Commun.* **2012**, 48, 8970.

[2] Wang, Y.; Ranasinghe, M. I.; Goodson, T. J. *Am. Chem. Soc.* **2003**, 125, 9562.

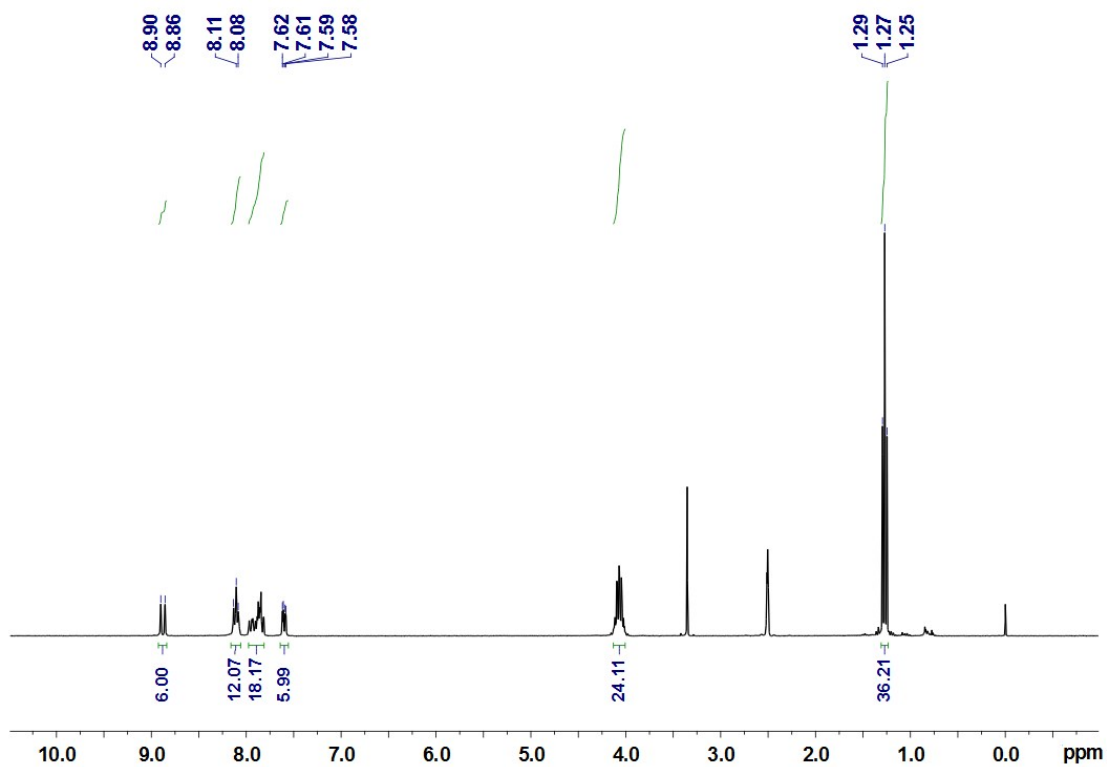


**Fig. S1**  $^1\text{H}$  NMR spectrum of TPPO in  $\text{DMSO-d}_6$ .

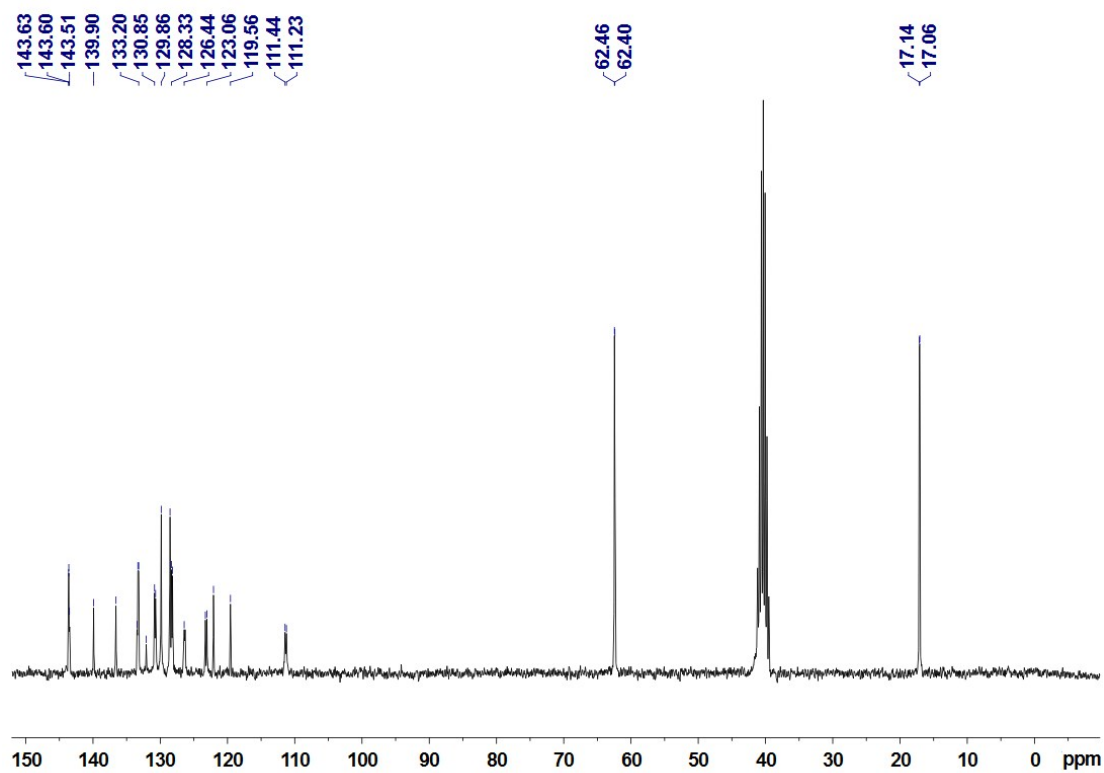


**Fig. S2**  $^{13}\text{C}$  NMR spectrum of TPPO in  $\text{DMSO-d}_6$ .

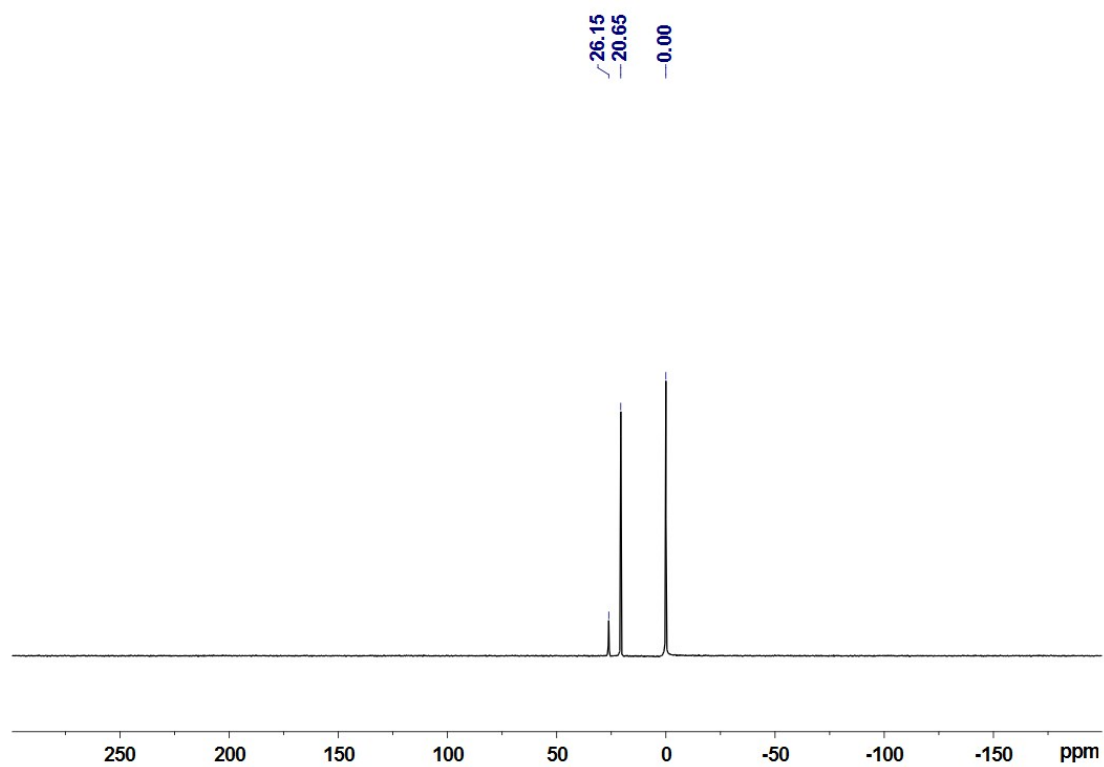


**Fig. S3**  $^{31}\text{P}$  NMR spectrum of TPPO in  $\text{DMSO-d}_6$  (0 ppm, 85% phosphoric acid in sealed capillary tube).

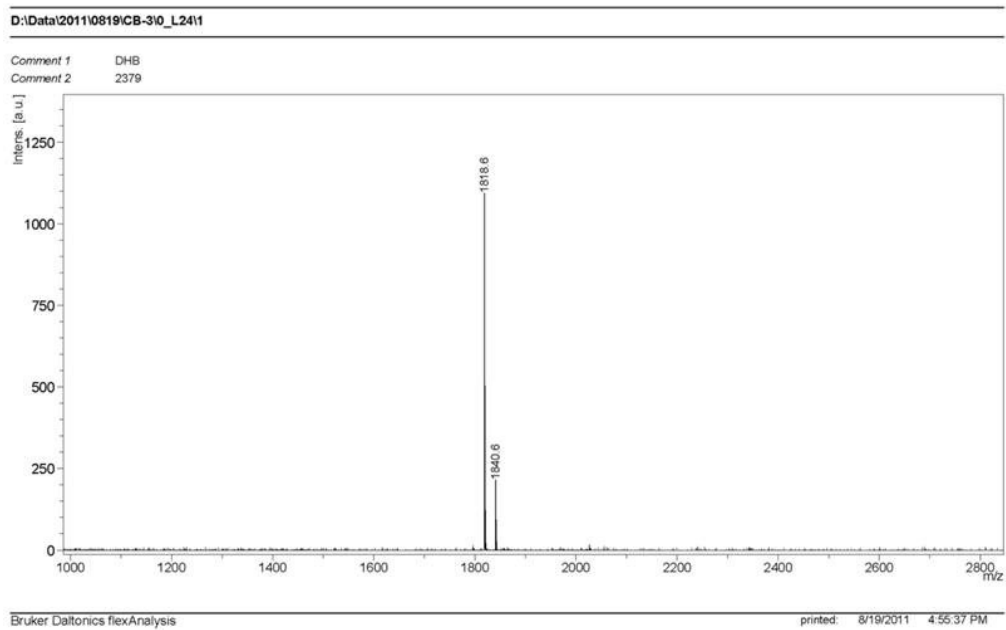


**Fig. S4** The MALDI-TOF mass spectrum of TPPO.



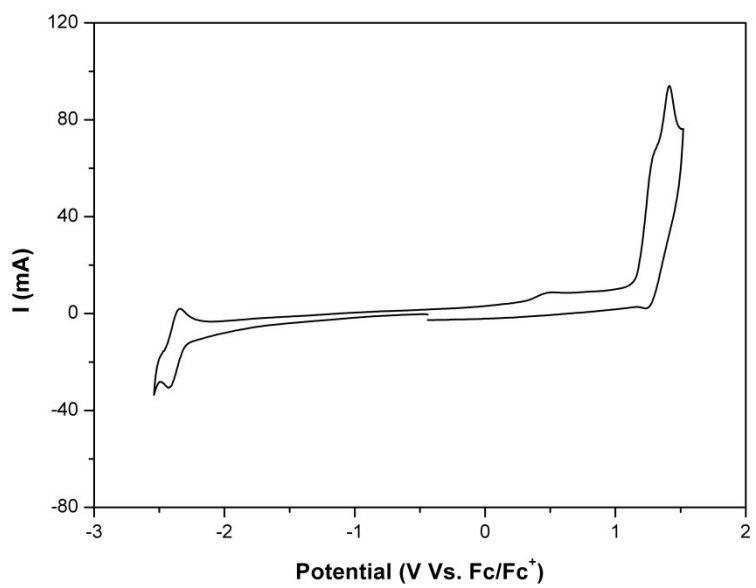


**Fig. S5** Cyclic voltammetry plot of TPPO in acetonitrile solution.

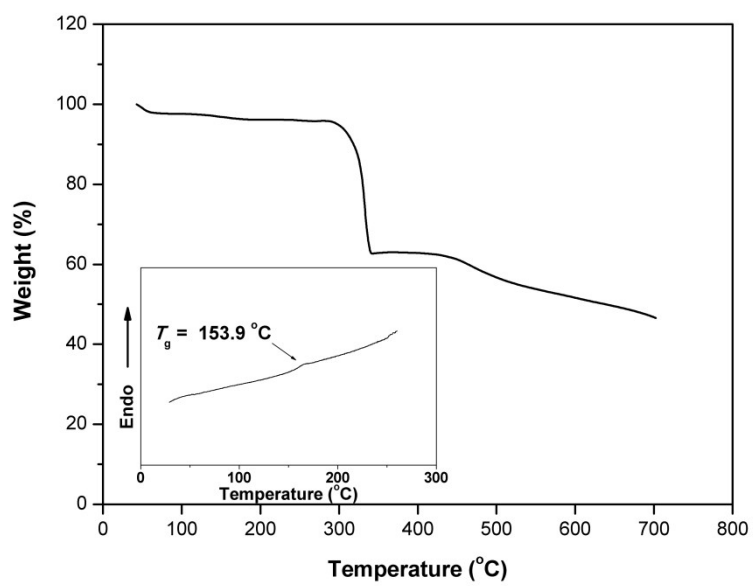


**Fig. S6** TGA and DSC curves (Inset: the second heating cycling) of TPPO

**Table S1** Photophysical, electrochemical and thermal properties of TPPO.

$\lambda_{\text{abs}} (\log \xi)^a$ [nm]	$\lambda_{\text{max}}^{\text{em}}^b$ [nm]	$E_g^c$ [eV]	$E_1^d$ [eV]	$E_{\text{ox}}^{\text{onset}}^e$ [V]	$E_{\text{red}}^{\text{onset}}^e$ [V]	HOMO <sup>e</sup> [eV]	LUMO <sup>e</sup> [eV]	$T_d^f$ [°C]	$T_g$ [°C]
243 (5.2), 249 (5.2), 269 (5.2), 286 (4.9), 307 (4.8)	371	3.49	2.65	1.16	-2.30	-5.96	-2.50	309	154

<sup>a</sup> Measured in 10<sup>-6</sup> M dichloromethane solution; <sup>b</sup> Measured in 10<sup>-6</sup> M toluene solution; <sup>c</sup> The optical band gap calculated from the onset of the absorption; <sup>d</sup> Measured in 10<sup>-3</sup> M toluene solution; <sup>e</sup> Measured in 10<sup>-3</sup> M acetonitrile solution, with *n*-5 Bu<sub>4</sub>NClO<sub>4</sub> as the electrolyte; <sup>e</sup> Calculated from the equations:  $E_{\text{HOMO}} = -e[E_{\text{ox}}^{\text{onset}} + 4.8 \text{ V}]$ ,  $E_{\text{LUMO}} = -e[E_{\text{red}}^{\text{onset}} + 4.8 \text{ V}]$ ; <sup>f</sup> The temperature of 5 % weight loss.

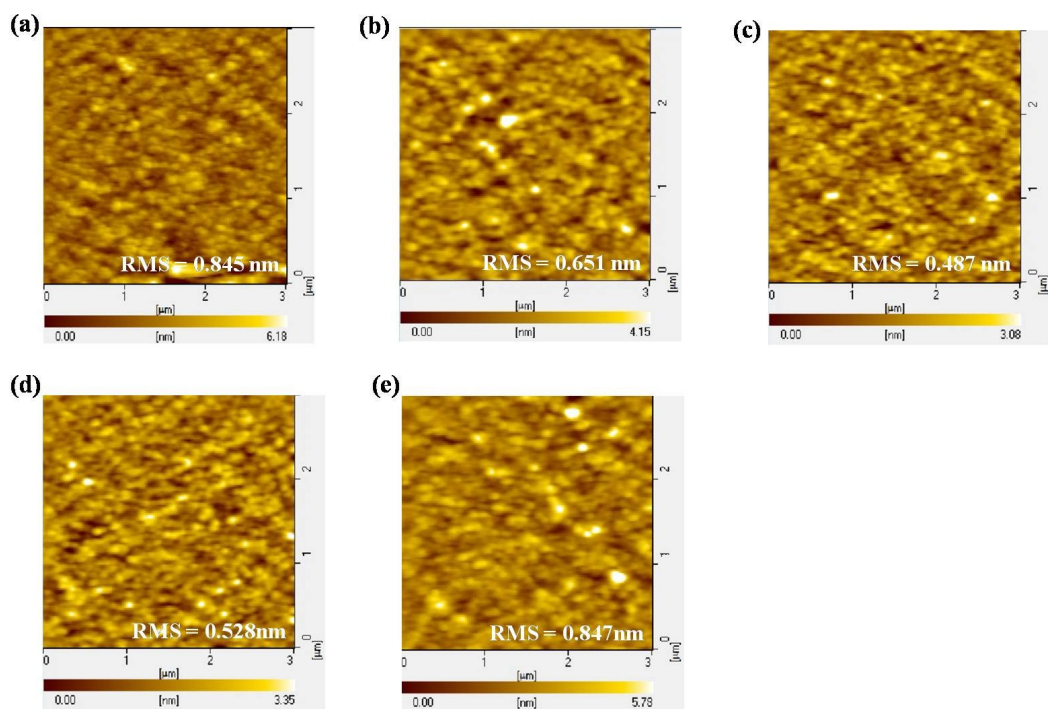


**Fig. S7** AFM surface topographic images for the TPPO film before (a) and after annealing at 120 °C for 1 h (b), 120 °C for 3 h (c), 120 °C for 5 h (d) and 140 °C for 5 h (e).

5

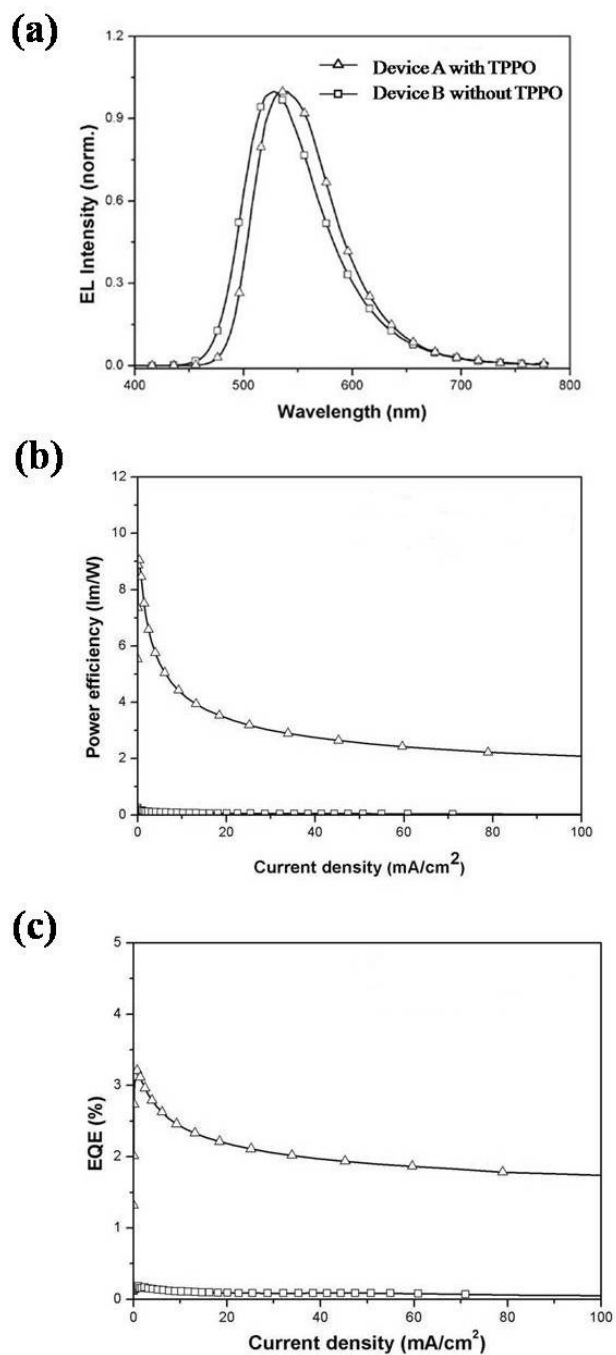


**Fig. S8** EL Spectra (a), power efficiency versus current density (b) and EQE versus current density plots (c) for devices with and without TPPO layer.

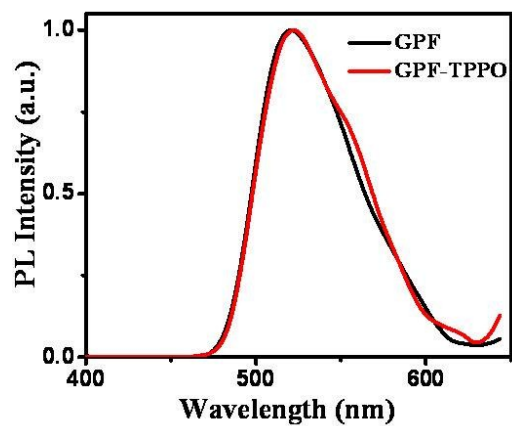


**Fig. S9** Comparison of the PL spectra for the GPF-composed EML before and after spin-coating of the upper TPPO layer.

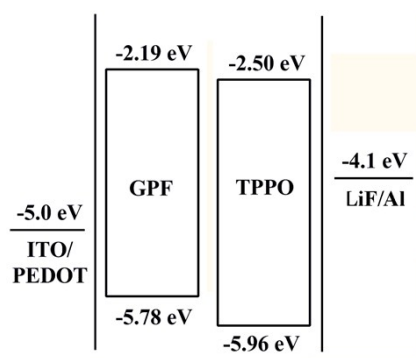


**Fig. S10** Energy level alignment of the multilayer device.

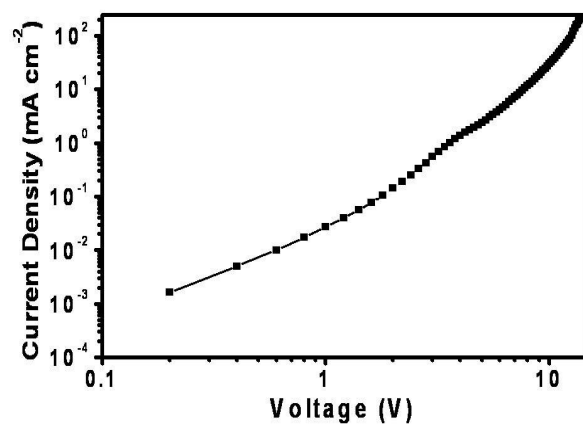


**Fig. S11** Current density-voltage plot of the electron-only device for TPPO.



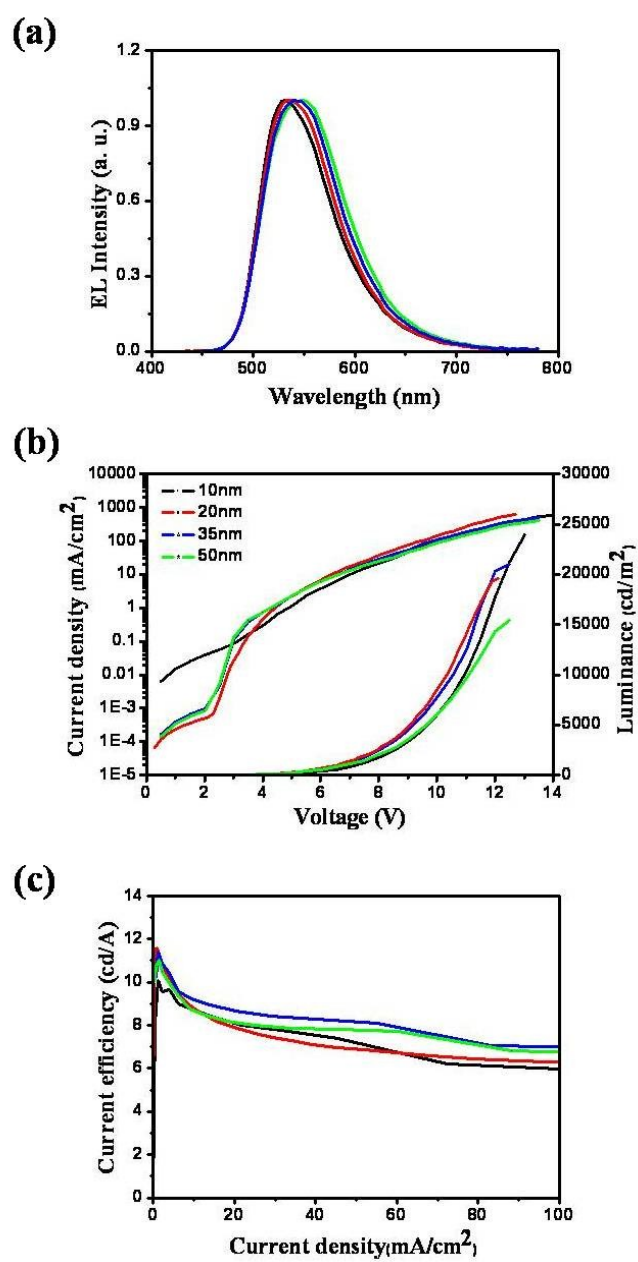


**Fig. S12** The EL spectra (a), current density-voltage-luminance (b) and current efficiency-current density characteristics for solution-processed multilayer PLEDs with different TPPO thickness.

---

**Table S2.** Device performance comparison for solution-processed multilayer PLEDs with different TPPO thickness.

Thickness [nm]	$V_{\text{on}}$ [V]	$L_{\text{max}}$ [cd m <sup>-2</sup> ]	$\eta_{\text{c, max}}$ [cd A <sup>-1</sup> ]	$\eta_{\text{p, max}}$ [lm W <sup>-1</sup> ]	$\text{EQE}_{\text{max}}$ [%]	$\lambda_{\text{max}}$ [nm]	CIE (x,y)
10	2.9	24000	10.0	6.3	2.8	531	0.35, 0.60
20	2.9	20000	11.6	9.1	3.2	540	0.36, 0.59
35	2.7	21000	11.3	8.0	3.2	543	0.37, 0.59
50	2.7	15000	11.0	7.7	3.1	551	0.38, 0.58